Volume 53 May 1988 Number 5

GEOPHYSICS

Ill-posedness of absorbing boundary conditions for migration

Louis H. Howell* and Lloyd N. Trefethen*

ABSTRACT

Absorbing boundary conditions for wave-equation migration were introduced by Clayton and Engquist. We show that one of these boundary conditions, the B2 (second-order) condition applied with the 45° (third-order) migration equation, is ill-posed. In fact, this boundary condition is subject to two distinct mechanisms of ill-posedness: a Kreiss mode with finite speed at one boundary and another mode of a new kind involving wave propagation at unbounded speed back and forth between two boundaries. Unlike B2, the third-order Clayton-Engquist boundary condition B3 is well-posed. However, we show that it is impossible for any boundary condition of Clayton-Engquist type of order higher than one to be well-posed with a migration equation whose order is higher than three.

INTRODUCTION

In 1980 Clayton and Engquist proposed a set of absorbing boundary conditions to minimize reflections at artificial boundaries in wave-equation migration (Clayton and Engquist, 1980). Migration involves a "one-way wave equation" with a semicircular dispersion relation (Claerbout, 1970), and so does the design of absorbing boundary conditions for ordinary wave-equation computations (Engquist and Majda, 1977). To construct absorbing boundary conditions for migration, Clayton and Engquist proposed combining both ideas in a quarter-circular dispersion relation. Their boundary conditions are now a standard, highly successful component of industrial calculations. For an introduction to these ideas, see the recent book by Claerbout (1985).

In this paper we show that one of the three Clayton-Engquist boundary conditions, the second-order condition they call B2, is ill-posed when applied in conjunction with the 45° migration equation. The ill-posedness is caused by two distinct mechanisms of wave propagation. One is a single-boundary effect of the kind identified by Kreiss (1970) for hyperbolic partial differential equations: a wave mode that may radiate physically spurious energy into the domain from the boundary. The other mechanism is a two-boundary effect that could not occur in a hyperbolic problem: a wave that reflects back and forth between two boundaries at an arbitrarily fast rate, growing at each reflection. Numerical experiments confirm that both of these mechanisms can cause certain model computations to fail.

Both forms of ill-posedness can occur in both time-domain and frequency-domain calculations. They are most likely to appear on computational grids fine enough to provide about ten or more points per wavelength. This may explain why the problem has apparently not been noticed before, although in any time-domain calculation or in any frequency-domain calculation in which a number of frequencies are superimposed, it is likely that some of the frequencies present will be low enough to lie in the dangerous range.

The two-boundary ill-posedness phenomenon addressed here is analogous to certain mechanisms of ill-posedness for hyperbolic partial differential equations in domains with corners which have been identified by Sarason and Smoller (1975) and Osher (1976). In these problems, unbounded growth of solutions results from arbitrarily rapid reflections of waves with finite speeds between two boundaries; the rapid reflections are possible because the distance between the boundaries

Manuscript received by the Editor January 5, 1987; revised manuscript received October 19, 1987.
*Department of Mathematics, Massachusetts Institute of Technology, Cambridge, MA 02139.

goes to zero at the corner. Here, in contrast, we have arbitrarily rapid reflections between boundaries a fixed distance apart, since the wave speeds of the 45° equation are unbounded.

Similar two-boundary ill-posedness phenomena might also occur in other problems involving an interior one-way wave equation, whether or not the boundary conditions are of the absorbing kind. For example, such phenomena may appear in underwater acoustics.

In the Appendix, we prove that the ill-posedness of the B2/45° combination is not exceptional; for a Clayton-Engquist boundary condition to be well-posed in conjunction with an interior migration equation, the orders of accuracy of both the boundary condition and the migration equation must not be too high.

CLAYTON-ENGQUIST BOUNDARY CONDITIONS

We confine our attention to a simple model problem: migration of upgoing acoustic waves in a two-dimensional (2-D) earth with constant sound speed equal to 1. Our results hold with little change for downgoing waves or a smoothly variable sound speed. Except for the presentation in terms of group velocity, the ideas of this section originated with Claerbout (1970) and Clayton and Engquist (1980).

The 2-D acoustic wave equation is $P_{tt} = P_{xx} + P_{zz}$, where x and z are the range and depth, t is time, and P is the wave amplitude. Substituting the plane wave $P(x, z, t) = e^{i(k_x x + k_z z - \omega t)}$ into this equation gives the dispersion relation $\omega^2 = k_x^2 + k_z^2$, or $k_z = \pm\omega(1 - k_x^2/\omega^2)^{1/2}$. The minus sign corresponds to upgoing waves, i.e., waves propagating in the $-z$ direction, so we have the following ideal dispersion relation for migration:

$$k_z = -\omega\sqrt{1 - k_x^2/\omega^2}. \tag{1}$$

Equation (1) describes a semicircle, but for finite-difference calculations, the square root must be approximated by a rational function $r(k_x/\omega)$, i.e., a quotient of polynomials in the variable k_x/ω:

$$k_z = -\omega r\left(\frac{k_x}{\omega}\right). \tag{2}$$

The two most common approximations are the Padé approximants

$$\text{Padé (2, 0):} \quad \sqrt{1 - k_x^2/\omega^2} \approx 1 - \tfrac{1}{2}k_x^2/\omega^2, \tag{3}$$

$$\text{Padé (2, 2):} \quad \sqrt{1 - k_x^2/\omega^2} \approx (1 - \tfrac{3}{4}k_x^2/\omega^2)/(1 - \tfrac{1}{4}k_x^2/\omega^2). \tag{4}$$

When these functions are inserted in equation (2), the resulting dispersion relations correspond to the following partial differential equations for migration:

$$\text{15° equation:} \quad P_{zt} = P_{tt} - \tfrac{1}{2}P_{xx}, \tag{5}$$

$$\text{45° equation:} \quad P_{ztt} = P_{ttt} - \tfrac{3}{4}P_{xxt} + \tfrac{1}{4}P_{xxz}. \tag{6}$$

Figure 1 shows the semicircle (1) and the approximations (2) based on equations (3) and (4). A variety of alternatives to Padé approximation are proposed in Halpern and Trefethen (1988).

In wave-equation migration, equation (5) or equation (6) is marched forward in the z direction by finite differences. Often a retarded time coordinate $t' = t + z$ is first introduced to eliminate the terms P_{tt} and P_{ttt}. It is also common to work with reduced equations in which a sinusoidal time dependence $e^{-i\omega t}$ or $e^{-i\omega t'}$ is assumed, so that time derivatives reduce to multiplications by $-i\omega$. This choice of frequency-domain or time-domain formulation has no effect on the mathematical derivations of ill-posedness in the rest of this paper.

The earth is essentially infinite in the $\pm x$ directions, but boundaries must be introduced for numerical computation, and these boundaries should be designed to generate minimal reflections of outgoing waves back into the computational domain. To make this idea precise, we can use the notion of group velocity, which is also the basis of the analysis of well-posedness. In the migration calculation, z is the "time" variable. Therefore, according to the theory of linear dispersive waves (Whitham, 1974), energy associated with the wavenumbers k_x and k_z travels at the group velocity

$$C = -\frac{\partial k_z}{\partial k_x}, \tag{7}$$

where velocity is interpreted as change in x per change in z. The partial derivative in equation (7) is obtained by differentiating the dispersion relation relating k_x, k_z, and ω. In other words, the group velocity equals the negative of the slope of the appropriate curve in Figure 1.

At a left-hand boundary $x = x_{\text{LEFT}}$, we want a boundary condition that admits only waves with $C < 0$, so that they will pass out of the computational domain. Clayton and Engquist observed that it is therefore appropriate to look for a boundary condition whose dispersion relation is a quarter-circle, the right half of the semicircle of Figure 1:

$$k_x = \omega\sqrt{1 - k_z^2/\omega^2}, \qquad k_z/\omega < 0. \tag{8}$$

Notice that here and subsequently, we switch from k_z to k_x as the dependent variable when describing boundary conditions. For a right-hand boundary, the sign in equation (8) is reversed.

Once again, the circular arc must be approximated by a rational function for finite-difference calculations. Clayton and Engquist proposed approximations in which the square root in equation (8) is replaced by a constant, linear, or hyperbolic

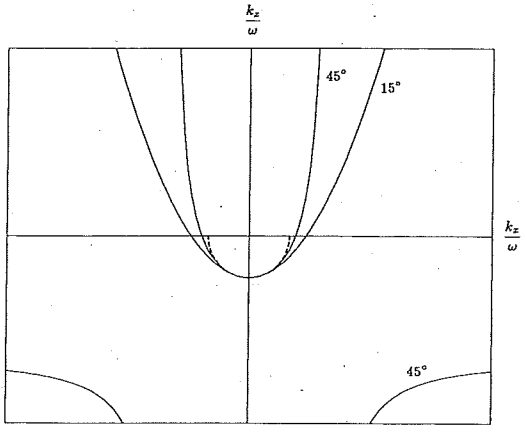

FIG. 1. Dispersion relations for migration of upgoing waves: ideal (dashed), 15° approximation, 45° approximation. The group velocity for propagation in x of a (k_x, k_z) wave during migration in the $+z$ direction is the negative of the slope of the dispersion relation.

function of k_z, as follows:

$$\sqrt{1 - k_z^2/\omega^2} \approx a, \tag{9}$$

$$\sqrt{1 - k_z^2/\omega^2} \approx b + ck_z/\omega, \tag{10}$$

$$\sqrt{1 - k_z^2/\omega^2} \approx \frac{d + ek_z/\omega}{1 + fk_z/\omega}. \tag{11}$$

From here on we use the coefficients $a = 1/2$, $b = 2 + \sqrt{3}$, $c = 2 + \sqrt{3}$, $d = 1$, $e = 1$, and $f = 2 - 2/\sqrt{3}$, which have been chosen so that the rational functions interpolate the quarter-circle at multiples of 30°. These approximations are illustrated in Figure 2. The differential equations corresponding to equations (9)–(11) are the following:

$$\text{B1:} \quad P_x = -aP_t, \tag{12}$$

$$\text{B2:} \quad P_x = -bP_t + cP_z, \tag{13}$$

$$\text{B3:} \quad -P_{xt} + fP_{xz} = dP_{tt} - eP_{zt}. \tag{14}$$

Altogether, a migration calculation consists of solving an interior equation (5) or (6) together with a boundary condition (12), (13), or (14) at the left-hand boundary, and an analogous equation with the x derivatives negated at the right-hand boundary. The numerical solution is carried out by finite-difference formulas, but since our ill-posedness results hold for the differential equations themselves, we do not specify a particular discretization until we turn to computational examples.

KREISS ILL-POSEDNESS

An initial boundary-value problem is well-posed if a unique solution exists for each set of initial and boundary data and depends continuously on these data. The precise definition depends upon what norms are used to measure the data, but except in certain borderline cases, a problem that is ill-posed in one norm is usually ill-posed in others, too. One cannot count on obtaining meaningful solutions to such problems.

In 1970, H.-O. Kreiss published a theory of well-posedness for hyperbolic initial boundary-value problems (Kreiss, 1970). The main result of Kreiss's theory is a well-posedness criterion that can be summarized as follows: a one-boundary problem is ill-posed if and only if, even in the absence of explicit forcing data at the boundary, it admits a solution consisting entirely of waves propagating inward from the boundary. The meaning of "inward" is defined in most cases by the group velocity. A two-boundary problem is well-posed if and only if each of its boundaries satisfies the Kreiss condition individually. See Higdon (1986) for a physical summary of the Kreiss theory, and Gustafsson et al. (1972) and Trefethen (1984) for analogous results on the stability of finite-difference discretizations.

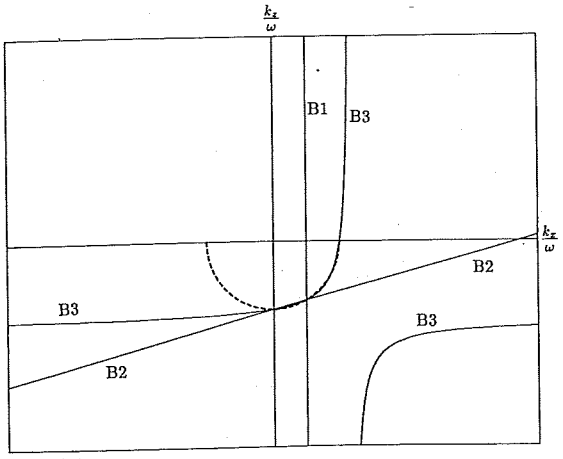

FIG. 2. Dispersion relations for absorbing boundary conditions at a left-hand boundary $x = x_{\text{LEFT}}$: ideal (right half of dashed semicircle), B1, B2, B3.

Our migration problem is not hyperbolic, and we do not know of a necessary and sufficient condition for well-posedness. The Kreiss criterion, however, is still necessary. That is, one can still look for incoming wave modes, and if there are any, the problem must be ill-posed. An incoming wave mode at a left-hand boundary is a wave $e^{i(k_x x + k_z z - \omega t)}$ that satisfies three conditions:

(1) k_x, k_z, ω satisfy the dispersion relation of the boundary condition;

(2) k_x, k_z, ω satisfy the dispersion relation of the interior equation; and either

(3a) *Propagating wave*: k_x, k_z, ω are real and $C > 0$, i.e., $\partial k_z/\partial k_x < 0$, for the interior equation, or

(3b) *Stationary wave*: ω is real and Im $k_z \le 0 <$ Im k_x.

In the Kreiss theory, condition (3a) is weakened to $C \ge 0$ to make the condition sufficient as well as necesary, but the ill-posedness associated with modes of type $C = 0$ is of a borderline kind in that they have negligible impact in migration problems. Condition (3b) does not come up in the examples we consider, nor, so far as we know, is it important in practical computations.

In other words, we must look for intersections of a curve from Figure 1 and a curve from Figure 2. If there is a point of intersection for which $\partial k_z/\partial k_x < 0$ in Figure 1, the problem is ill-posed.

Consider first the B1 boundary condition. Superimposing Figures 1 and 2 by eye, we see that there is just one intersection point of the B1 line with the dispersion curve for the 15° or 45° equation, and this point has $\partial k_z/\partial k_x > 0$. Thus we have no evidence of ill-posedness. In fact, in the appendix to their paper, Clayton and Engquist prove the stability of a finite-difference discretization of the B1 condition with the 15° equation, which implies well-posedness of the differential equation.

Similarly, the B3 boundary condition admits no Kreiss ill-posed wave modes in combination with the 15° or 45° wave equations in the interior, except for the mode $k_x = 0$, which is of the borderline sort with $C = 0$.

With the B2 condition and the 45° equation, however, an ill-posed intersection point appears on one of the outer branches of the dispersion relation for the 45° equation, with $k_x/\omega \approx -7.97$ for our standard choice of b and c in equation (13). This point represents a plane wave with wave crests at the angle $\approx 21.5°$ from the z-axis, propagating to the right from the boundary with the modest group velocity $C \approx 0.036$ (see Figure 3). This wave is entirely an artifact of the rational approximation of our one-way wave operators, not being physically related to the original migration problem at all.

We conclude

Theorem 1. *The B2 boundary condition is ill-posed in combination with the 45° migration equation.*

Theorem 1 is valid for any choice of b and c in equations (10) and (13), provided $c \neq 0$. One can make the theorem

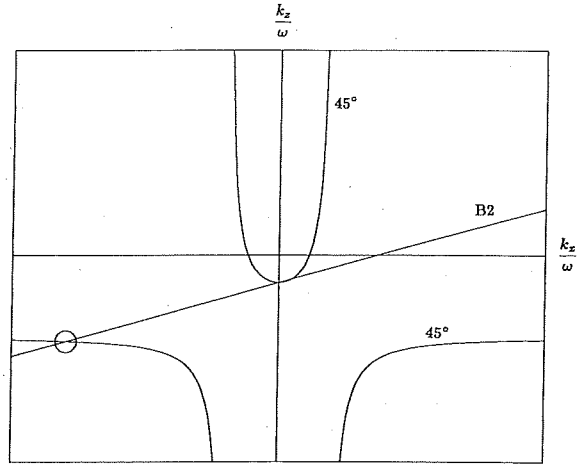

FIG. 3. Superimposed dispersion relations for the 45° migration equation and the B2 boundary condition. The circled intersection point corresponds to an ill-posed mode of Kreiss type that propagates inward from a left-hand boundary.

quantitative in various ways by using asymptotic methods of group velocity analysis (cf., Trefethen, 1984, for the discrete case). Kreiss discusses this matter on p. 72 of Kreiss (1974), where he considers a "generalized eigenvalue of the second kind" for an ill-posed hyperbolic example. The ill-posed mode has the effect that, at best, one must expect a "loss of one derivative." That is, to ensure that no dangerous nonphysical reflections from the boundary occur, as a minimum one must take wave data that are smooth. In the next section we show that the situation is actually worse than this.

TWO-BOUNDARY ILL-POSEDNESS

In our first numerical experiments on coarse meshes, the ill-posed mode of the last section had no visible effect. It began to appear when we made the mesh finer, and unexpectedly, we also began to encounter another phenomenon of ill-posedness that is often more pronounced. The key to these results is reflection coefficients.

To calculate a reflection coefficient at a left-hand boundary, we begin with an incident plane wave $e^{i(k_x x + k_z z - \omega t)}$ that satisfies the migration equation and has group velocity $C < 0$. For either of the equations of Figure 1, this means that k_x, k_z, and ω satisfy the migration dispersion relation with $k_x > 0$. When such a wave hits the boundary, it generates a reflected plane wave in which k_z and ω have the same value, but k_x is negated. Therefore, we look for a linear combination

$$P(x, z, t) = A_L e^{i(k_x x + k_z z - \omega t)} + A_R e^{i(-k_x x + k_z z - \omega t)} \qquad (15)$$

that satisfies the boundary condition as well as the migration equation. To find such a linear combination, we insert equation (15) into the boundary condition and calculate $R = A_R/A_L$. The results are as follows:

$$\text{B1:} \quad R = \frac{k_x - a\omega}{k_x + a\omega}, \qquad (16)$$

$$\text{B2:} \quad R = \frac{k_x - b\omega - ck_z}{k_x + b\omega + ck_z}, \qquad (17)$$

$$\text{B3:} \quad R = \frac{k_x\omega - d\omega^2 - ek_z\omega + fk_x k_z}{} \qquad (18)$$

These functions are plotted for the 45° equation in the interior in Figure 4. For the B1 and B3 conditions, R is bounded, and indeed $|R(k_x)| \le 1$ for all k_x. However, the plot for the B2 condition is dominated by a pole at $k_x/\omega \approx 7.97$. This "infinite reflection coefficient" corresponds to the ill-posed mode identified in the last section.

Figure 4 suggests that for the B2/45° combination, the wavenumber $k_x/\omega \approx 7.97$ will dominate. In fact, though, the wavenumber $k_x/\omega = 2$ often turns out to be more important since the group velocity C becomes infinite there. The formula for C as a function of k_x/ω, obtained via equation (7) by differentiating the dispersion relation that results from equations (2) and (4), is

$$C = \frac{-k_x/\omega}{(1 - \frac{1}{4}k_x^2/\omega^2)^2}. \qquad (19)$$

Figure 5 plots $|C|$ as a function of k_x/ω.

In a migration calculation with two absorbing boundaries, the following will happen. Wave energy for a given value k_x hits the left-hand boundary and is amplified by $|R(k_x)|$. Then it propagates to the right at a speed of $|C(k_x)|$ until it hits the right-hand boundary, where it is amplified again by the same factor, and so on. If L is the distance between the boundaries,

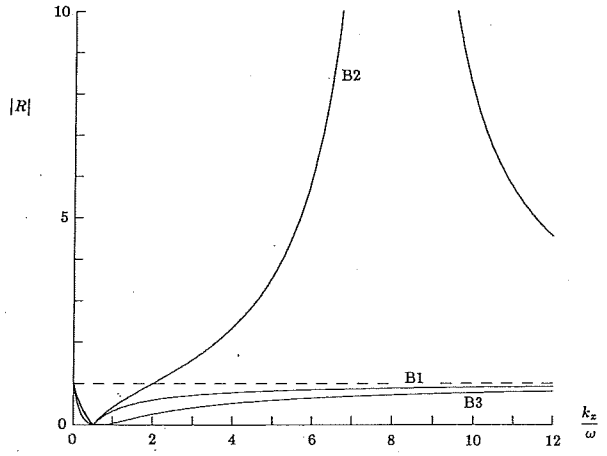

FIG. 4. Reflection coefficients $|R|$ as functions of k_x/ω for the 45° equation with boundary conditions B1, B2, B3.

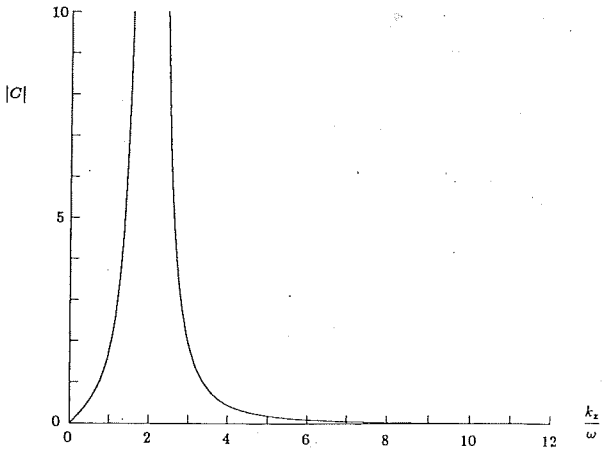

FIG. 5. Group speed $|C|$ as a function of $k_x\omega$ for the 45

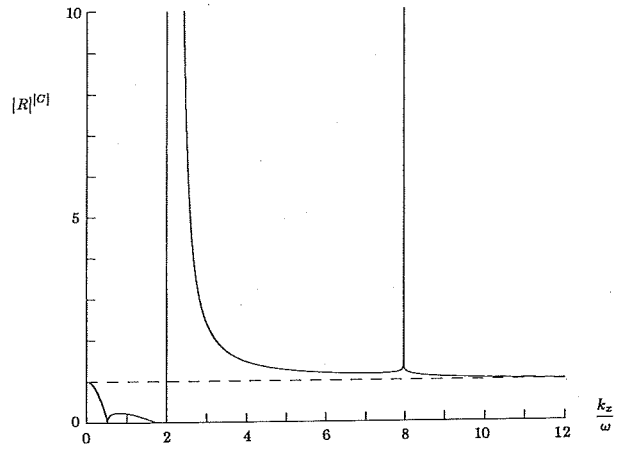

FIG. 6. $|R|^{|C|}$ as a function of k_x/ω for the 45° equation with boundary condition B2. This quantity determines the rate of energy growth due to two-boundary interactions.

this back-and-forth process results in a growth in amplitude at the rate

$$A(z) \approx |R(k_x)|^{|C(k_z)|z/L}. \tag{20}$$

Note that z/L behaves here like a normalized time variable.

Figure 6 plots the crucial quantity $|R|^{|C|}$ as a function of k_x/ω. The singularity at $k_x/\omega \approx 7.97$ is still present, but a much stronger singularity has appeared at $k_x/\omega = 2$, even though $|R|$ approaches 1 at that point. This singularity at $k_x/\omega \approx 2$ is capable of creating a tremendous growth of energy.

We can make the behavior near $k_x/\omega \approx 2$ quantitative as follows. Consider a wave mode with $k_x/\omega = 2 + \varepsilon$ for small $\varepsilon > 0$. We get

$$|R|^{|C|} = \left[1 + O(\varepsilon)\right]^{O(\varepsilon^{-2})} = e^{O(\varepsilon^{-1})}, \tag{21}$$

where the O means "order of." This function of ε has not merely a pole, but an essential singularity at $\varepsilon = 0$. In a finite-difference discretization, this will translate into an instability that gets exponentially worse as the mesh is refined at a rate $e^{O(h^{-1})}$, where h is the grid size. The Kreiss instability associated with $k_x/\omega \approx 7.97$, in contrast, will worsen at the much more modest (algebraic) rate $O(h^{-1})$.

FINITE-DIFFERENCE FORMULAS

Following Clayton and Engquist, we solved the 45° equation in retarded time in the frequency domain by an implicit Crank-Nicolson type finite-difference formula:

$$(\omega^2 \delta_+^z + \tfrac{1}{4}\delta_2^x \delta_+^z + \tfrac{1}{2} i\omega \delta_2^x \mu_+^z)P = 0, \tag{22}$$

where δ_+ is a forward difference, δ_2 is a second-order centered difference, and μ_+ is a forward average. The Clayton-Engquist boundary conditions were discretized as

$$\text{B1:} \quad \left[\delta_+^x - ia\omega\mu_+^x\right]P = 0, \tag{23}$$

$$\text{B2:} \quad \left[c\mu_+^x \delta_+^z - \delta_+^x \mu_+^z - i\omega(c-b)\mu_+^x \mu_+^z\right]P = 0, \tag{24}$$

$$\text{B3:} \quad \left[ie\omega\mu_+^x \delta_+^z - f\delta_+^x \delta_+^z - i\omega(1-f)\delta_+^x \mu_+^z + \omega^2(e-d)\mu_+^x \mu_+^z\right]P = 0. \tag{25}$$

Discretization affects the analysis described in the last section considerably. Let Δx, Δz be the step sizes in x and z. For the continuous problem, we have the dispersion relations

$$45°: \quad \frac{k_z}{\omega} = -(\omega^2 - \tfrac{3}{4}k_x^2)/(\omega^2 - \tfrac{1}{4}k_x^2), \tag{26}$$

$$\text{B2:} \quad \frac{k_x}{\omega} = b + c\frac{k_z}{\omega}, \tag{27}$$

and the corresponding reflection coefficient and group velocity functions were listed in equations (17) and (19). With the discretizations in equations (22) and (24), these formulas become

$$45°: \quad \omega\Delta z \cot\left[\tfrac{1}{2}(k_z + \omega)\Delta z\right] - (\omega\Delta x)^2 \csc^2(\tfrac{1}{2}k_x\Delta x) + 1 = 0, \tag{28}$$

$$\text{B2:} \quad c \tan\left[\tfrac{1}{2}(k_z + \omega)\Delta z\right]\Big/(\omega\Delta z) - \tan(\tfrac{1}{2}k_x\Delta x)/(\omega\Delta x) - \tfrac{1}{2}(c-b) = 0, \tag{29}$$

and, after a good deal of algebra,

$$C = -\frac{2\cos\left(\frac{1}{2}k_x\Delta x\right)\sin^2\left[\frac{1}{2}\left(k_z + \omega\right)\Delta z\right]\Big/(\omega\Delta z)^2}{\sin^3\left(\frac{1}{2}k_x\Delta x\right)\Big/(\omega\Delta x)^3}, \tag{30}$$

$$R = \frac{2\tan\left(\frac{1}{2}k_x\Delta x\right)\Big/(\omega\Delta x) - (b-c) - 2c\tan\left[\frac{1}{2}\left(k_z + \omega\right)\Delta z\right]\Big/(\omega\Delta z)}{2\tan\left(\frac{1}{2}k_x\Delta x\right)\Big/(\omega\Delta x) + (b-c) + 2c\tan\left[\frac{1}{2}\left(k_z + \omega\right)\Delta z\right]\Big/(\omega\Delta z)} \tag{31}$$

Because of aliasing, these functions have periods of $2\pi/\omega\Delta x$ in k_x/ω and $2\pi/\omega\Delta z$ in k_z/ω.

Figure 7 indicates the effect of the finite mesh by plotting $|R|^{|C|}$, as in Figure 6, for nine pairs of values $\omega\Delta x$, $\omega\Delta z$. As explained in the last section, the peak in the plots near $k_x/\omega = 2$ is due to large group velocities there, although they are no longer infinite on the discrete mesh, while the singularity at higher k_x/ω is due to an infinite reflection coefficient. Reading horizontally across the figures shows that as $\omega\Delta x$ increases for fixed $\omega\Delta z$, the dominant effect is that the Kreiss ill-posed mode moves to a smaller wavenumber. It also be-

comes more pronounced, largely because C increases, although the figure does not show this in the most appropriate way, since $|R|^{|C|}$ is a measure of two-boundary interactions. At $\omega\Delta x = 1$, the Kreiss mode ceases to exist, and the difference model is stable for $\omega\Delta x \geq 1$, although not very accurate. On the other hand, reading vertically down the figure shows that $\omega\Delta z$ has a dominant effect on the two-boundary ill-posed mode. For $\omega\Delta z \approx 0$, the function $|R|^{|C|}$ is nearly singular at $\omega\Delta x = 2$, although not actually singular as in the continuous case. As $\omega\Delta z$ increases, the group velocity goes down and $|R|^{|C|}$ rapidly diminishes.

Different discretizations would have different effects on R, C, and $|R|^{|C|}$ from those described in equations (30)–(31) and in Figure 7. Any discretization, however, will give rise to periodic functions R, C, and $|R|^{|C|}$ that approach the curves of Figures 4–6 as the mesh becomes finer.

NUMERICAL EXPERIMENTS

Our numerical experiments involved two kinds of initial data at $z = 0$: random complex numbers uniformly distributed in the unit disk, the same for each experiment, and a smooth pulse obtained by superimposing seven frequencies, modeled after Figure 4 of Clayton and Engquist (1980). Real seismic data would lie between these two extremes of regularity. In each case we solved the discretization in equation (22) of the 45° equation on a domain with width 1, depth 2, and $\Delta x = \Delta z$, in single precision (7–8 digits) on a Sun workstation.

Figure 8 presents four calculations with random initial data on a 160×80 grid. Figures 8a–8c cut diagonally across Figure 7 from the lower right to the upper left, showing various values of ω with $\omega\Delta x = \omega\Delta z = 1, 0.6, 0.2$. These three plots illustrate the range of stability phenomena that we have

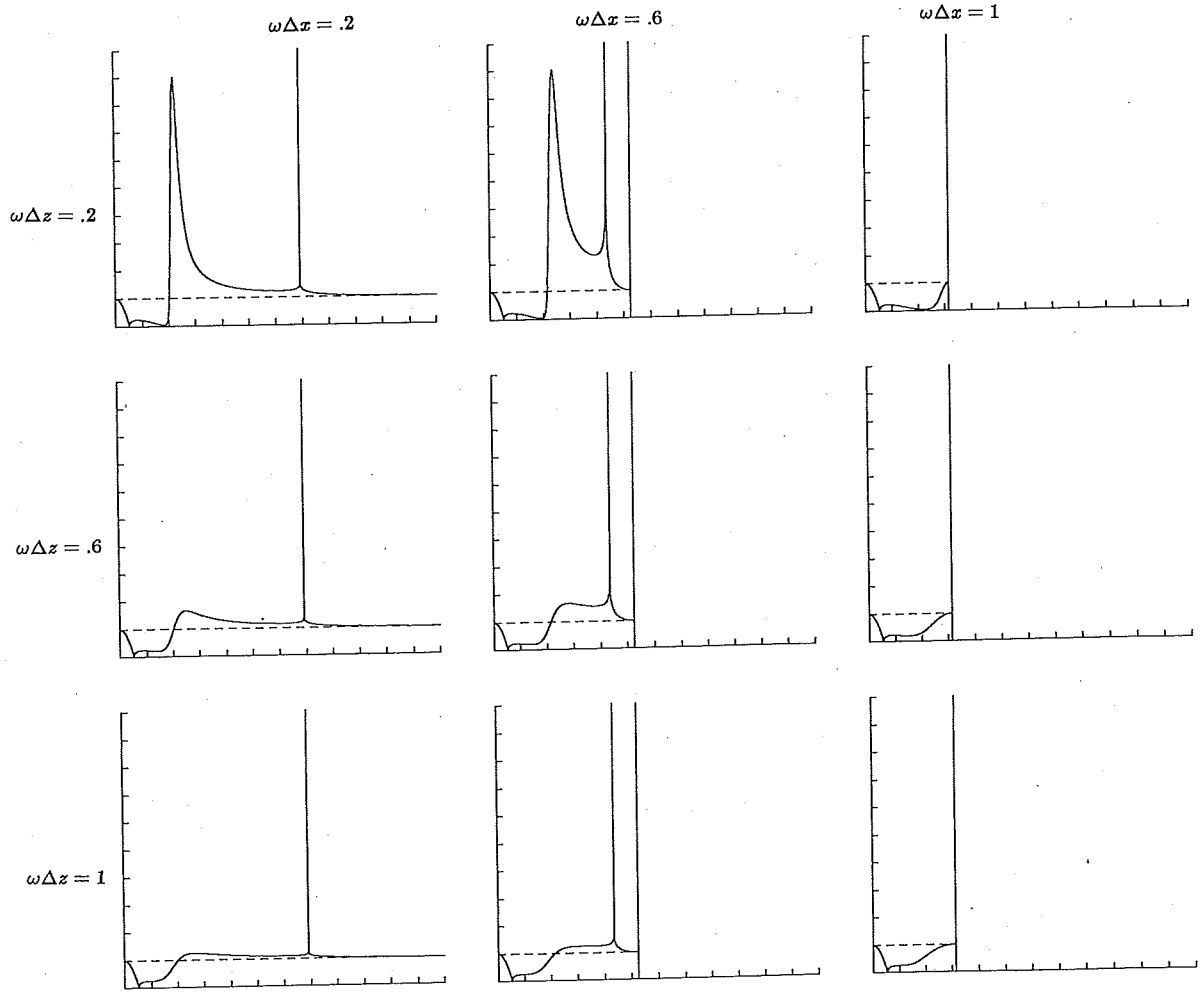

FIG. 7. $|R|^{|C|}$ as a function of k_x/ω for the discretized 45° equation and boundary condition B2, various $\omega\Delta x$ and $\omega\Delta z$. The vertical bars on the right (off-scale for $\omega\Delta x = 0.2$) indicate the largest wavenumbers representable on the grid.

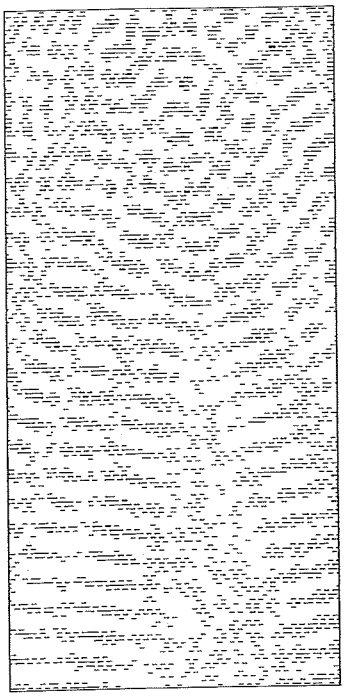

(*a*) B2, $\omega\Delta x = \omega\Delta z = 1$

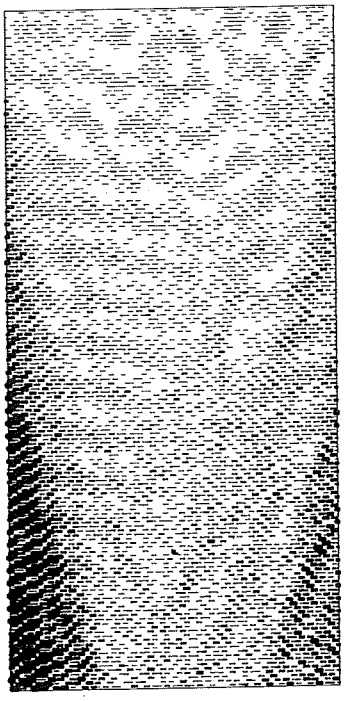

(*b*) B2, $\omega\Delta x = \omega\Delta z = .6$

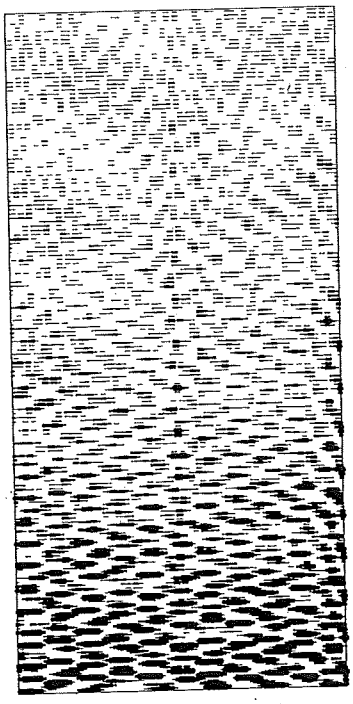

(*c*) B2, $\omega\Delta x = \omega\Delta z = .2$

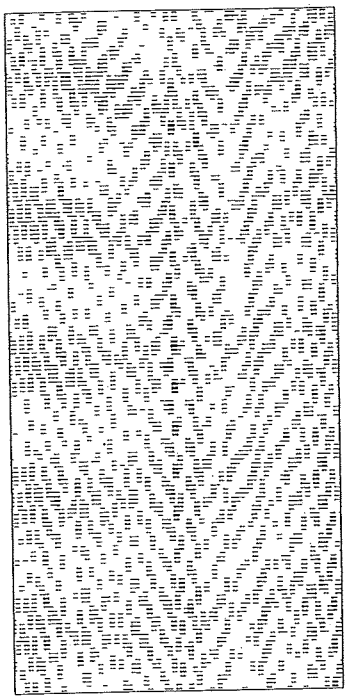

(*d*) B3, $\omega\Delta x = \omega\Delta z = .2$

FIG. 8. 45° migration calculations with random initial data on a 160 × 80 grid, various boundary conditions and frequencies.

described. In Figure 8a, ω is sufficiently large that no instability appears. In Figure 8b, the Kreiss instability is evident in the form of noise propagating in linearly from both boundaries. (The asymmetry between the two boundaries is a consequence of the random initial data.) In Figure 8c there is a hint of the Kreiss instability again, but it is soon obliterated by a much larger two-boundary instability. Obviously the latter two computations are unacceptable. Figure 8d repeats 8c, but with B2 replaced by the presumably well-posed boundary condition B3. The instabilities vanish.

Figure 9 quantifies these results. Figure 9a shows the rms energy as a function of z for the same four calculations as in Figure 8, revealing marked energy growth in the two unstable cases. Of the two stable calculations, the reason the B2/$\omega\Delta x = 1$ combination exhibits faster decay of energy than the B3/$\omega\Delta x = 0.2$ combination is that the group velocities are larger, so that more energy passes out through the boundaries (see Figure 8a).

Figure 9b shows the energy at fixed depth $z = 2$ for various values of $\omega\Delta x = \omega\Delta z$; each point of this plot was obtained from a separate calculation. As $\omega\Delta x$ decreases, the first bump in the B2 energy curve reflects the Kreiss instability, while the more catastrophic growth for $\omega\Delta x \leq 0.3$ represents the two-boundary effect. The more detailed structure of the data is a consequence of randomness and is not significant.

In both parts of Figure 9, the data for the B1 condition look almost the same as for the B3 condition and are therefore omitted.

Finally, Figure 10 shows a set of results modeled after Figure 4 of Clayton and Engquist. Each plot shows a superposition of calculations at seven different frequencies (multiples of $\omega = 24$). Not knowing the exact definition of Clayton and Engquist's wave function, we took initial data corresponding to a wave pulse of the form $\sin r \cos^{15} r$ centered at a point at a distance 0.1 above the middle of the domain. Figure 10a shows this computation on a 160×80 grid (minimum $\omega\Delta x = 0.3$), and Figure 10b shows it on a 320×160 grid (minimum $\omega\Delta x = 0.15$), both with the B2 boundary condition. The first computation appears stable, while the second is clearly unstable. In their paper, Clayton and Engquist present results for only B1 and B3, but it appears that their grid was closer to that of Figure 10a than Figure 10b, so a B2 calculation would have looked good also. Making the grid finer, however, is obviously dangerous.

Figure 10c repeats the computation on the 320×160 grid with the B3 boundary condition. Now the result is evidently stable, and in addition, the spurious reflections of Figure 10a have been nearly eliminated.

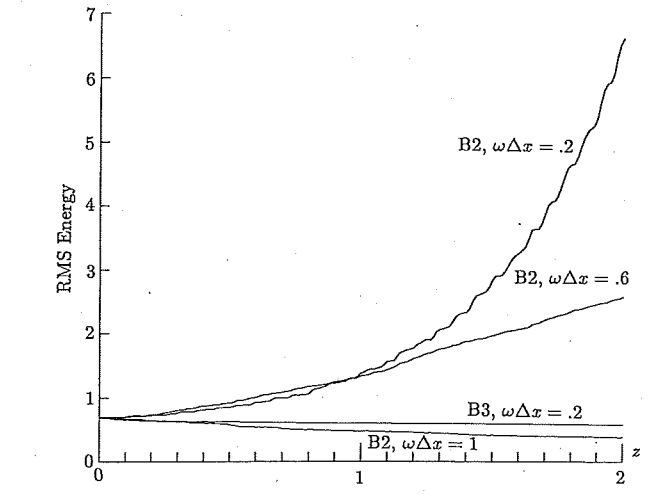

(a) Dependence on z

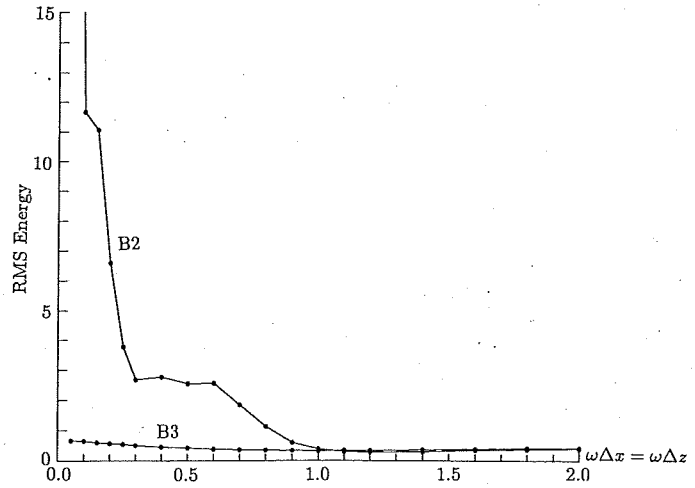

(b) Dependence on $\omega\Delta x = \omega\Delta z$ at fixed $z = 2$

FIG. 9. Computed rms energy as a function of z and $\omega\Delta x = \omega\Delta z$ for boundary conditions B2 and B3.

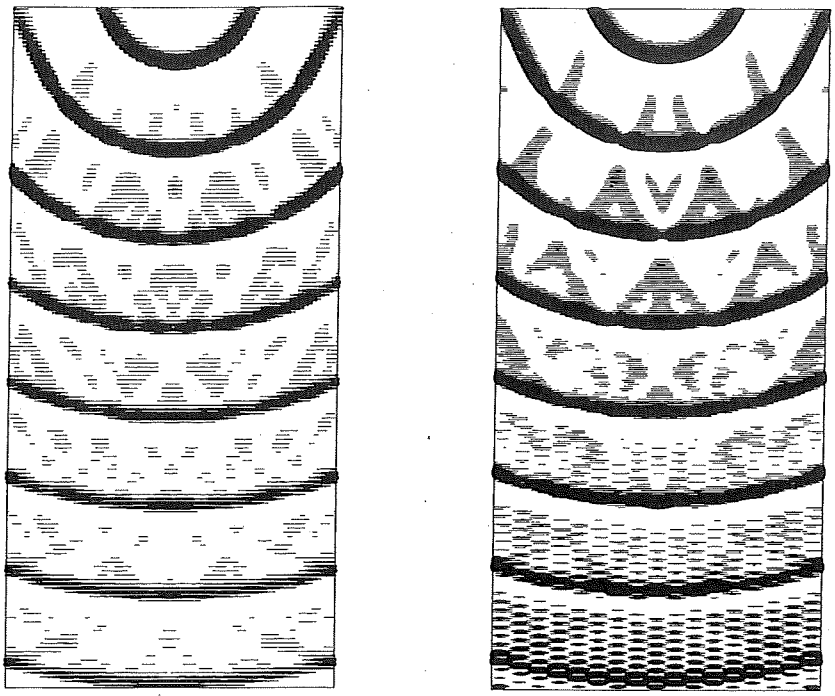

(*a*) B2, 160 × 80 grid

(*b*) B2, 320 × 160 grid

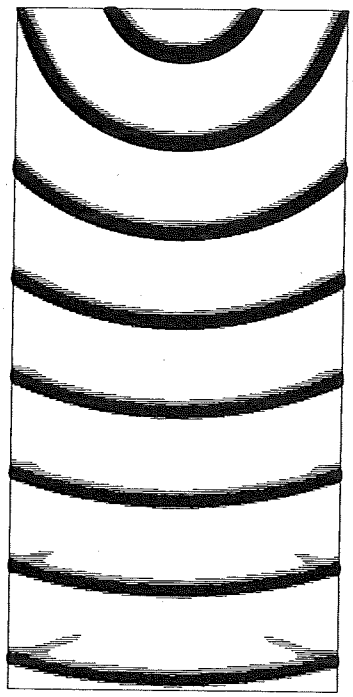

(*c*) B3, 320 × 160 grid

FIG. 10. 45° seven-frequency migration calculations with a base frequency of $\omega = 24$ (after Clayton and Engquist, 1980).

CONCLUSIONS

We have shown theoretically and by numerical experiments that the combination B2/45° (the B2 Clayton-Engquist boundary condition coupled with the 45° migration equation) is ill-posed. As proven in the Appendix, the same is true of any combination that has a higher order of accuracy than B3/45°. Therefore, we recommend the B3/45° combination whenever its implementation is convenient.

ACKNOWLEDGMENTS

LNT is happy to acknowledge a summer at Cambridge University (1985) with Michael Powell and Arieh Iserles, Department of Applied Mathematics and Theoretical Physics, during which this project began. Our results related to Kreiss ill-posedness were worked out with the help of Iserles.

REFERENCES

Claerbout, J. F., 1970, Coarse grid calculations of waves in inhomogeneous media with application to delineation of complicated seismic structure: Geophysics, **35**, 407–418.
——— 1985, Imaging the earth's interior: Blackwell Scientific Publ.
Clayton, R. W., and Engquist, B., 1980, Absorbing boundary conditions for wave equation migration: Geophysics, **45**, 895–904.
Dahlquist, G., 1963, A special stability problem for linear multistep methods: BIT, **3**, 27–43.
Engquist, B., and Majda, A., 1977, Absorbing boundary conditions for the numerical simulation of waves: Math. Comput., **31**, 629–651.
Gustafsson, B., Kreiss, H.-O., and Sundström, A., 1972, Stability theory of difference approximations for initial boundary value problems. II: Math. Comput., **26**, 649–686.
Halpern, L., and Trefethen, L. N., 1988, Wide-angle one-way wave equations: J. Acoust. Soc. Am., to appear.
Higdon, R. L., 1986, Initial-boundary value problems for linear hyperbolic systems: Soc. Industr. Appl. Math. Review, **28**, 177–217.
Kreiss, H.-O., 1970, Initial boundary value problems for hyperbolic systems: Comm. Pure Appl. Math., **23**, 277–298.
Kreiss, H.-O., 1974, Boundary conditions for hyperbolic differential equations, Proc., Dundee Conference on Numerical Solution of Differential Equations, Lect. Notes in Math. 363, Springer-Verlag, New York, Inc.
Osher, S., 1976, Hyperbolic equations in regions with characteristic boundaries or with corners, *in* Hubbard, B., Ed., Numerical solution of partial differential equations III: Academic Press Inc.
Sarason, L., and Smoller, J. A., 1975, Geometrical optics and the corner problem: Arch. Rat. Mech. Anal., **56**, 34–69.
Trefethen, L. N., 1984, Instability of difference models for hyperbolic initial boundary value problems: Comm. Pure Appl. Math., **37**, 329–367.
Trefethen, L. N., and Halpern, L., 1986, Well-posedness of one-way wave equations and absorbing boundary conditions: Math. Comput., **47**, 421–435.
Whitham, G. B., 1974, Linear and nonlinear waves: John Wiley and Sons, Inc.

APPENDIX

A WELL-POSEDNESS BARRIER

In this Appendix we show that well-posed migration formulas with absorbing boundary conditions of the Clayton-Engquist kind can only have a limited order of accuracy: the B3/45° combination is the best possible. Our argument is based on identifying Kreiss ill-posed modes. This result is mainly of theoretical interest, since B3 and 45° are accurate enough for most purposes. If it were important to obtain higher-order approximations, well-posed variations on the Clayton-Engquist theme could very likely be devised.

Consider a migration formula derived from a dispersion relation as in equation (2),

$$\frac{k_z}{\omega} = -r\left(\frac{k_x}{\omega}\right), \tag{A-1}$$

where r is a rational function of exact type $(2m, 2n)$, i.e., it has numerator of degree $2m$ and denominator of degree $2n$ [equation (1)]. We assume that r is an even function, i.e., $r(-s) = r(s)$, that $r(0) \in (0, \infty)$, that $r(s)$ interpolates $+\sqrt{1-s^2}$ at $2m + 2n + 2$ points of $(-1, 1)$, counted with multiplicity, and that $n \le m \le n + 1$. All of the equations used in practice satisfy these conditions (Trefethen and Halpern, 1986). The order of the migration formula is defined to be its order as a partial differential equation, namely, $d = m + n + 1$. The 5°, 15°, and 45° equations have multiple interpolation points at $s = 0$ and orders $d = 1, 2, 3$, respectively.

By an absorbing boundary condition of Clayton-Engquist type, we mean a boundary condition derived from a dispersion relation as in equations (8)–(11),

$$\frac{k_x}{\omega} = R\left(\frac{k_z}{\omega}\right), \tag{A-2}$$

where R is a rational function of exact type (M, N) [equation (8)]. We assume that $R(S)$ interpolates $+\sqrt{1-S^2}$ at $M + N + 2$ points of $[-1, 1]$, counted with multiplicity, or $M + N + 1$ points if $M + N$ is odd, that $R(0) \in (0, \infty)$, and that $N \le M \le N + 2$. The order of the boundary condition is defined to be $D = M + N + 1$; its order as a differential equation is $(D + 1)/2$ if $M + N$ is even, or $D/2$ if $M + N$ is odd (Trefethen and Halpern, 1986). The boundary conditions B1, B2, and B3 satisfy these conditions with $D = 1, 2, 3$, respectively.

We now consider a migration initial boundary-value problem consisting of the interior equation derived from equation (A-1) together with at least one left-hand boundary on which the boundary condition derived from equation (A-2) is applied. Although far more specialized, the following result is analogous to Dahlquist's theorem in numerical analysis which states that no A-stable linear multistep formula for discretization of ordinary differential equations can have an order of accuracy greater than two (Dahlquist, 1963).

Theorem 2. *The initial boundary-value problem described above must be ill-posed if it has interior order $d \ge 4$ and boundary condition order $D \ge 2$.*

Proof. By lemmas 1 and 2 of Trefethen and Halpern (1986), $r(s)$ must have the form

$$r(s) = a - cs^2 + \sum_{k=1}^{n} \frac{b_k s^2}{s^2 - s_k^2}, \tag{A-3}$$

with $a > 0$, $c \geq 0$, $b_k > 0$ for $k \geq 1$, and $1 < s_1 < s_2 < \cdots < s_n < \infty$. The coefficient c will be zero if $m = n$, nonzero if $m = n + 1$. Similarly, $R(S)$ must have the form

$$R(S) = A + BS - CS^2 + \sum_{k=1}^{N} \frac{B_k S}{S - S_k}, \tag{A-4}$$

with $A > 0$, B arbitrary, $C \geq 0$, $B_k > 0$ for $k \geq 1$, and $-\infty < S_1 < S_2 < \cdots < S_N < \infty$.

If $d \geq 4$, then either $n \geq 2$, or $n = 1$ and $c > 0$. In either case, equation (A-3) implies that the graph of $-r(s)$ contains at least one component with $s < 0$ that runs from $+\infty$ to $-\infty$ with negative slope, which corresponds to a positive group velocity. Similarly, if $D \geq 2$, then equation (A-4) implies that the graph of $R(S)$ contains at least one component that runs from a positive value to $-\infty$. When the graphs of $-r(s)$ and $R(S)$ are superimposed with s and S at right angles to each other, as in Figure 3, the two components of $-r(s)$ and $R(S)$ just mentioned must intersect somewhere. This point of intersection corresponds to a Kreiss ill-posed wave.